

Research Report – Forschungsbericht

Lanthanides as d Metals

Arndt Simon*, Hansjürgen Mattausch, Mikhail Ryazanov, and Reinhard K. Kremer

Stuttgart, Max Planck-Institut für Festkörperforschung

Received December 21st, 2005.

Professor Hansgeorg Schnöckel zum 65. Geburtstag gewidmet

Abstract. Reduction of lanthanide trihalides with alkali metals along the route used by *Klemm* and *Bommer* leads to pure lanthanide metals. In closed Ta capsules at elevated temperatures, however, metal-rich halides form which use the excess of Ln centered electrons for metal-metal bonding. An overview of the extended d metal chemistry of lanthanides in binary, ternary and quaternary

halides is presented. Consequences of the mutual interaction of d and f electrons are illustrated for selected magnetic and electrical properties.

Keywords: Lanthanides; Lanthanide halides; Reduction by alkali metals

Introduction

One of the numerous important scientific achievements of *Wilhelm Klemm* was the discovery of the periodic behaviour of 4 f elements [1]. *Klemm* explained the occurrence of the oxidation states +2 and +4 besides the main one, +3, for the lanthanides Ln in terms of specific electronic configurations. Lanthanum in its oxidation state +3 has an empty 4 f shell, in the Ln³⁺ ions of gadolinium and lutetium – the latter called cassiopeium in those days – the 4f shell is half-filled and fully occupied, respectively. The immediate neighbours easily adopt these stable configurations, too, the preceding ones by forming Ln²⁺ ions like europium and ytterbium and the following ones by forming Ln⁴⁺ ions as in the cases of cerium and terbium. In order to reach these textbook results *Klemm* and *Bommer* [1] reduced minute amounts of the respective trichlorides with alkali metals. Micro-crystalline rare earth metals formed besides alkali metal chloride which served as an internal standard in the x-ray measurements. In the detailed description of the experiments one finds the remark: “Unstimmigkeiten in der Analyse, d.h. unvollkommene Umsetzung, drückten sich in den Röntgendiagrammen stets durch flauere Filme und das Auftreten von Fremdlinien aus.” This remark raises the question whether *Klemm* and *Bommer* witnessed the existence of still further reduced lanthanide halides below ox-

idation state +2, discovered several decades later with Gd₂Cl₃ [2, 4] and many more to come [4, 5, 6].

Our article is composed of three parts. At first we describe experiments along the line of the investigations of *Klemm* and *Bommer* corroborating the early results. Secondly, we briefly review the structures of halides which contain lanthanide metals in low oxidation states. The structural chemistry closely relates to that of heavy d metals with clusters and condensed clusters and heralds a novel d metal chemistry of the lanthanides. The fascinating back and forth interaction of d and f electrons in these compounds will be addressed in the third part.

1 Reduction of lanthanide halides by alkali metals

As Gd₂Cl₃ is quite easily accessible, gadolinium is our target metal to seek for the formation of a metal-rich compound following the experimental procedure of *Klemm* and *Bommer* [1]. We added varying amounts of potassium to GdCl₃ and heated the reactants in evacuated and sealed glass ampoules to temperatures between 520 K and 720 K. Only the lower part of the ampoule was introduced into the furnace, and excess K condensed in the cold upper part. After approximately a day the reaction product in all experiments consisted of a black top layer of Gd and KCl sharply separated by a white layer of unreacted GdCl₃. Only that part of GdCl₃ which was wetted by molten K was reduced but no reduction of the remaining part with gaseous K occurred. Even the contact region between the two layers did not contain traces of Gd₂Cl₃. Obviously, the formation of elemental Gd happens much faster than that of the metal-rich compound. Performing the reaction in a quasi “open system” at moderate temperature as *Klemm*

* Prof. Dr. A. Simon
Max-Planck-Institut für Festkörperforschung
Heisenbergstr. 1
D-70569 Stuttgart
Fax: +49 711 689 1642
E-mail: A.Simon@fkf.mpg.de

and *Bommer* did leads to pure and well crystallised metal. The same result is obtained, when GdCl_3 and Na are reacted at 520 K in uniformly heated sealed Ta capsules which results in Gd and NaCl besides unreacted GdCl_3 . However, at higher temperatures, 620 to 720 K, partial reduction to Gd_2Cl_3 is observed in such a “closed system” after several days together with the formation of ternary Na-Gd-Cl phases [7].

It lies at hand to prepare other metal-rich Ln halides by reduction with alkali metals and, indeed, Gd_2Br_3 , Tb_2Cl_3 and Tb_2Br_3 could be made along this metallothermic route [8]. This route is of particular interest as a fast high yield way to prepare LaI , the first true Ln monohalide, which was recently identified in a mixture of La and LaI_3 after long-term annealing [9]. However, reacting stoichiometric amounts of Na with LaI_3 in a closed Ta capsule at 820 K always results in a contamination of the product by La. Only the use of LaI_2 , possibly via intercalation into the layered crystals, leads to LaI with no traces of La detectable [10]. The difference clearly indicates the relevance of kinetics in the reduction reactions.

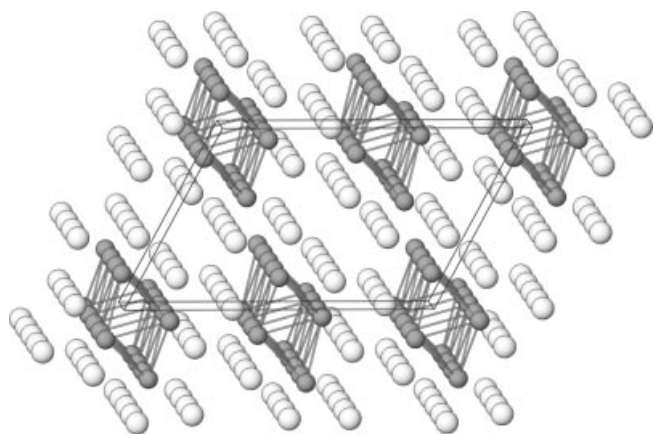


Fig. 1 Parallel projection of the crystal structure of Gd_2Cl_3 along [010], unit cell outlined, Gd atoms dark.

2 Metal-rich lanthanide halides

The dihalides of Ln metals provide the essential feature of bonding with the growing class of metal-rich compounds formed by these metals. Whereas the dihalides of Eu and Yb are normal Ln^{2+} salts as mentioned in the introduction, the metal atoms in LaI_2 or GdI_2 adopt the preferred configurations f^0 and f^7 , respectively, as Ln^{3+} ions, and the excess electrons reside in conduction bands with d character. Thus, the metallic dihalides are closely related with corresponding compounds of the heavy d transition metals. The similarity is quite striking as e.g. for the isovalence-electronic and isotopic pair GdI_2 and TaS_2 .

The structural chemistry of metal-rich compounds of 4 d and 5 d elements is characterised by the frequent occurrence of discrete and condensed metal clusters [11, 12]. Many different cluster topologies are known out of which

the M_6X_{12} cluster with an octahedral core is somewhat dominating in the case of the valence electron poor metals

Table 1 Compounds and structural units in M-M bonded halides of Sc, Y, Ln with interstitial atoms Z.

Ln₆ octahedra		
discrete clusters		
$\text{Ln}_7\text{ZX}_{12}$	single octahedra	[22]
$\text{La}_6(\text{C}_2)\text{I}_{10}$	single octahedra	[23]
$\text{CsEr}_6\text{Cl}_{12}$	single octahedra	[24]
$\text{Sc}_6\text{C}_2\text{I}_{11}$	single octahedra	[25]
$\text{Y}_6\text{RuI}_{10}$	single octahedra	[26]
$\text{CsY}_{10}(\text{C}_2)_2\text{I}_{18}$	single octahedra	[27]
$\text{Gd}_{10}(\text{C}_2)_2\text{Cl}_{18}$	double octahedra	[28]
$\text{CsEr}_{10}(\text{C}_2)_2\text{I}_{18}$	double octahedra	[29]
$\text{Er}_{10}(\text{C}_2)_2\text{I}_{18}$		
$\text{Gd}_{10}(\text{C}_2)_2\text{Cl}_{17}$	double octahedra	[28]
$\text{Gd}_{10}(\text{C}_2)_2\text{I}_{16}$	double octahedra	[30]
$\text{Tb}_{10}\text{B}_2\text{Br}_{15}$	double octahedra	[30]
$\text{La}_{10}\text{Os}_2\text{I}_{15}$	double octahedra	[31]
$\text{La}_{10}(\text{C}_2)_2\text{I}_{15}$	double octahedra	[23]
$\text{Cs}_2\text{La}_{10}\text{Co}_2\text{I}_{17}$	double octahedra	[32]
$\text{Cs}_2\text{Pr}_6(\text{C}_2)_2\text{I}_{12}$	double octahedra	[33]
$\text{La}_{14}(\text{C}_2)_3\text{I}_{20}$	triple octahedra	[34]
$\text{Tb}_{16}\text{B}_4\text{Br}_{23}$	quadruple octahedra	[35]
$\text{Y}_{20}\text{Ir}_4\text{Br}_{36}$ (= Y_5IrBr_9)	quadruple octahedra	[36]
chains		
$\text{Ln}_4\text{CX}_5\text{-Typ}$	linear single chains	[37]
$\text{Ln}_4\text{ZX}_6\text{-Typ}$	linear single chains	[38, 39]
$\text{Gd}_4(\text{C}_2)(\text{Cl}, \text{I})_6$	linear single chains	[40]
$\text{Ln}_4\text{B}_4\text{X}_5\text{-Typ}$	linear single chains	[41]
Sc_5CCl_8	linear single chains	[42]
Tb_4BBr_6	angular single chains	[43]
$\text{Tb}_{13}\text{B}_3\text{Br}_{18}$	linear chain + double octahedra	[44, 45]
$\text{Ln}_6\text{C}_2\text{X}_7$	double chains	[12]
Gd_3Cl_3	double chains	[46]
Pr_3RuI_3	double chains	[47]
$\text{Sc}_7\text{C}_2\text{Cl}_{10}$	double chains	[48]
$\text{Y}_{10}\text{C}_2\text{I}_{13}$	single and double chains	[49]
sheets		
Ln_2CX	planar sheets	[15]
Gd_2CHBr	planar sheets	[50]
Gd_2CHCl		
Ln_2HX_2	planar sheets	[51, 52]
Ln_2CX_2	planar sheets	[53, 54, 55]
$\text{Ln}_2\text{C}_2\text{X}_2$	planar sheets	[53, 56]
$\text{Ln}_2\text{H}_4\text{X}_2$	planar sheets	[57]
$\text{Gd}_4\text{C}_2\text{X}_3$	undulated sheets	[58]
$\text{Gd}_6\text{C}_3\text{Cl}_5$	undulated sheets	[59]
frameworks		
La_3AuI_3	3D nets	[60]
La_3GaBr_3	3D nets	[61, 62]
Ln₄ tetrahedra		
Gd_3NCl_6	double tetrahedra	[63]
$\text{Gd}_2\text{Cl}_3\text{N}$	chains	[64]
Ln₆ octahedra and Ln₄ tetrahedra		
Gd_4CNI_6	chains of double tetrahedra and octahedra	[65]
$\text{Y}_6\text{C}_2\text{NI}_9$	chains of double tetrahedra and double octahedra	[65]
$\text{Y}_7\text{C}_3\text{OI}_6$	sheets of 3 double octahedra and 1 tetrahedron	[66]
$\text{Y}_9\text{C}_4\text{OI}_8$	sheets of 4 double octahedra and 1 tetrahedron	[67]
$\text{Y}_{16}\text{C}_7\text{O}_2\text{I}_{14}$	combination of 3/4 double octahedra + 2 tetrahedra	[68]

Table 1 (continued).

Ln ₆ trigonal prisms		
around B		
Ce ₃ (BC)Br ₃	single chains	[41]
Y ₁₆ (B ₂ C ₄) ₂ I ₁₉	double chains (B-C groups)	[69]
Pr ₈ B ₇ Cl ₇	double chains (B ₈ , B ₆ , B ₃ , B ₂)	[70]
Y ₂₁ (BC ₂) ₇ I ₁₈	flat sheets	[71]
La ₉ (BC ₂) ₃ Br ₅	undulated sheets (C-B-C groups)	[72]
La ₉ (BC ₂) ₃ Br ₆	undulated sheets (C-B-C groups)	[41]
Gd ₄ (BC)CBr ₃	undulated sheets, prisms and octahedra (B-C, C)	[73]
Ce ₆ (BC) ₂ CBr ₃	undulated sheets, prisms and octahedra (C-B-B-C, C)	[73]
around Si		
La ₃ Si ₃ Cl ₂	sheets (Si-zig-zag chains)	[74]
La ₆ Si ₇ Br ₃	sheets (strand of Si ₁₂ rings)	[74]
CeSiI	sheets (flat sheets of Si ₆ rings)	[75]
La ₄ Si ₄ I ₃	sheets (undulated sheets of Si ₆ , Si ₁₄ rings)	[75]
La ₅ Si ₅ I ₃	sheets (sheets of Si ₂₂ rings)	[75]
around Al		
La ₂ Al ₂ I	flat sheets (Al ₆ sheets)	[60]
La ₃ Al ₂ I ₂	undulated sheets (Al ₆ chains)	[60]
Ce ₂₉ Al ₁₄ I ₂₈	undulated sheets and double octahedra (Al ₆ chains, isolated Al atoms)	[76]
La ₁₀ Al ₅ I ₈	undulated sheets and chains of octahedra (chains of Al ₆ -rings, isolated Al atoms)	[77]
La ₂₄ Al ₁₂ I ₂₁	strands (Al ₆ chains)	[77]
Ln ₅ trigonal bipyramids		
La ₅ (C ₂)I ₉	single bipyramids	[23, 78]
M ₅ (C ₂)Cl ₉ (M=La, Pr)	single bipyramids	[78]
RbPr ₅ (C ₂)Cl ₁₀	single bipyramids	[79]

Nb and Ta. With these metals the M₆ octahedron is empty, however, a further decrease of the number of available metal valence electrons (e.g. with Zr or Th) weakens the homonuclear M-M bonding which has to be compensated for by strong heteronuclear bonds with interstitial (endohedral) atoms. It therefore does not come as a surprise that in the case of the Ln metals with even less valence electrons these clusters are nearly always stabilised by interstitial atoms. Only a few binary Ln halides with M-M bonding exist. These are the earlier mentioned layered dihalides LaI₂, CeI₂, PrI₂ and GdI₂ [13]. LaI crystallises in a NiAs-type structure though with such a large *c/a* ratio that this phase, too, constitutes rather a two-dimensional metallic system. The compounds Ln₂X₃ can be viewed as condensed cluster phases. The structure of Gd₂Cl₃ shown in figure 1 exhibits the feature of chains of empty trans-edge-sharing Gd₆ octahedra surrounded by halogen atoms, and the excess metal valence electrons reside mainly in strong localised M-M bonds within the shared edges. The compound is a semiconductor, hence, the M-M bonds are localised.

The number of M-M bonded halides which contain additional atoms is quite large and still keeps growing. Examples are listed in table 1. Only selected structures will be shown in the following figures which are reduced to characteristic building units instead of presentations of the entire crystal structures. Figure 2 summarises discrete clusters derived from the M₆X₁₂ prototype which contain endohedral atoms or C₂ units. The clusters with cores of one to four

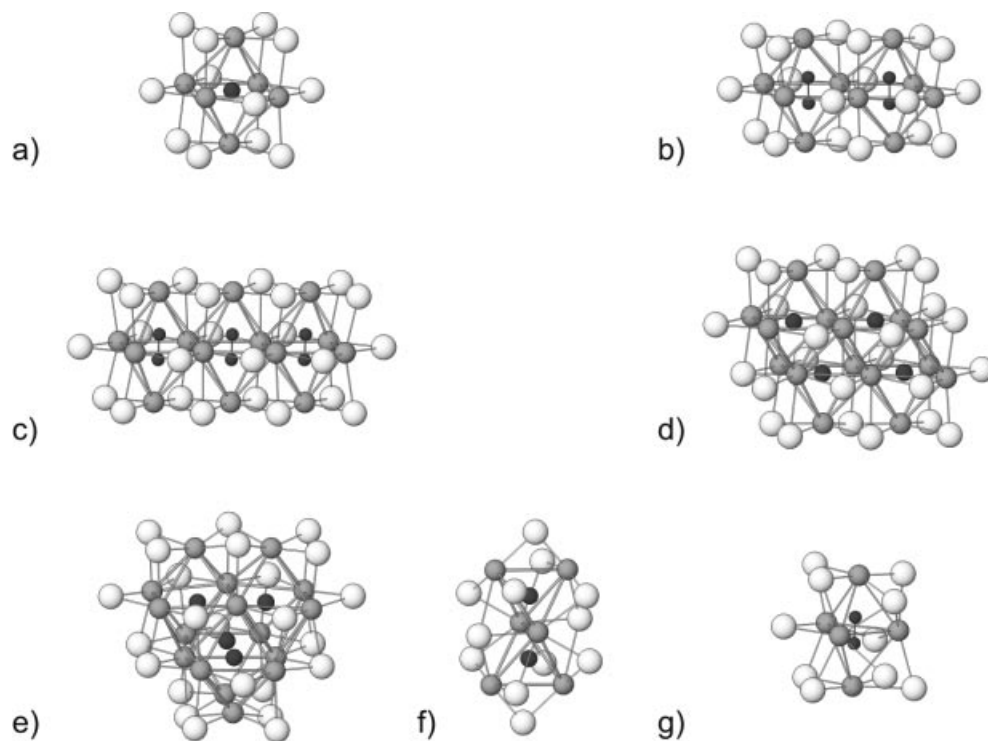


Fig 2 Discrete clusters in Sc, Y and Ln halides (halogen, metal and interstitial atoms (B, C, N), respectively, drawn with decreasing size); (a-e) shows the single Ln₆ZX₁₂ cluster together with units formed by its condensation; (f, g) display units formed from two Ln₄Z tetrahedra by condensation via edges and faces, respectively.

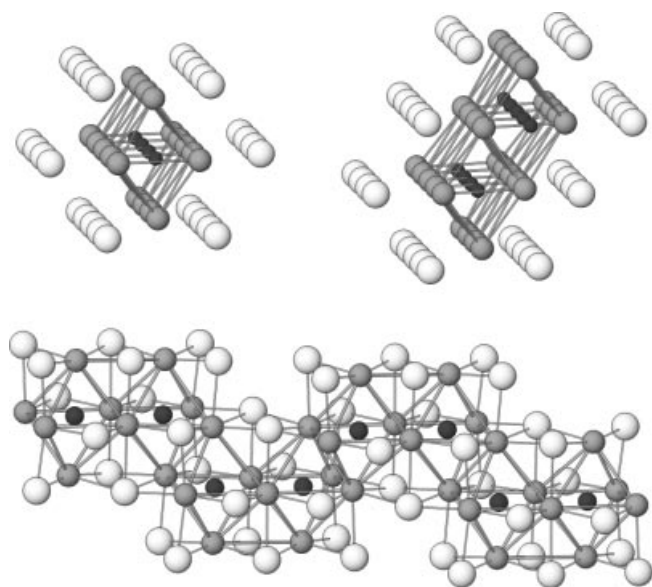


Fig. 3 Chains of condensed Ln_6Z octahedra, atoms drawn as in figure 2.

Ln_6 octahedra are found in a variety of different structures. One should note that some of these clusters, namely those containing one to three octahedra, also occur with reduced oxomolybdates, however, with empty octahedra there due to the larger number of valence electrons available with Mo. Of course, cluster chemistry with lanthanides as also experienced with d transition metals is not confined to octahedral Ln_6 units. Figure 2 also shows alternatives like e.g. Ln_4 tetrahedra condensed via edges or faces in Ln_6 and Ln_5 units, respectively.

Some of the clusters shown in figure 2 constitute the building blocks of infinitely extending frameworks. Examples of increasing dimensionality are given in the next figures. In figure 3, linear as well as zig-zag chains are shown which due to variations in their interconnections comprise a remarkably large class of crystal structures. In addition, different building units can be combined as illustrated for some nitride carbide halides in figure 4. The structural features are preserved in the next step of condensation which leads to two-dimensional networks. Planar layers of condensed Ln_6 octahedra closely relate to corresponding crystal structures with d transition metals. However, whereas the monohalides of Zr exist as binary compounds the Ln compounds with this atomic arrangement need the stabilisation by additional atoms inserted into the octahedra. Hydrogen atoms are particularly interesting as their concentration can be reversibly adjusted within certain limits. Figure 5 indicates that M-M bonding occurs in LnH_nX within the range of homogeneity, $0.67 \leq n \leq 1.00$, and is lost upon full hydrogenation to LnH_2X . Other than H atoms are found as interstitial entities, e.g. C atoms or C_2 units bonded as methanide and ethenide ions, respectively. (Ethanide ions are frequently found in other C_2 containing phases.) Layers Ln_2CX_2 form compounds with the very same composition, or, when linked via X atoms, compounds of composition Ln_2CX . As mentioned above with one-dimensional structures, the combination of different building blocks offers nearly unlimited possibilities in the case of two-dimensional (and three-dimensional) structures, too. Figure 6 is just a glimpse into the variations of structures exemplified with oxide carbide halides of the rare earth metal Y which is a “true” d metal and forms numerous metal-rich compounds similar to the lanthanides.

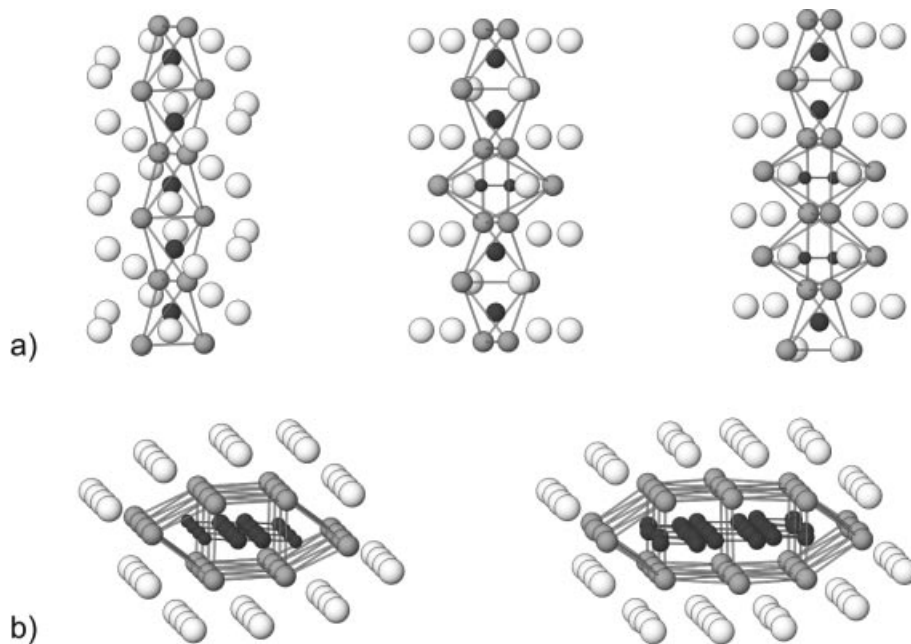


Fig. 4 Chains of condensed Ln_4Z tetrahedra and Ln_6Z octahedra (top) in nitride carbide halides and chains of Ln_6Z prisms and Ln_5Z pyramids (bottom) in boride carbide halides; atoms drawn as in figure 2, C atoms smallest.

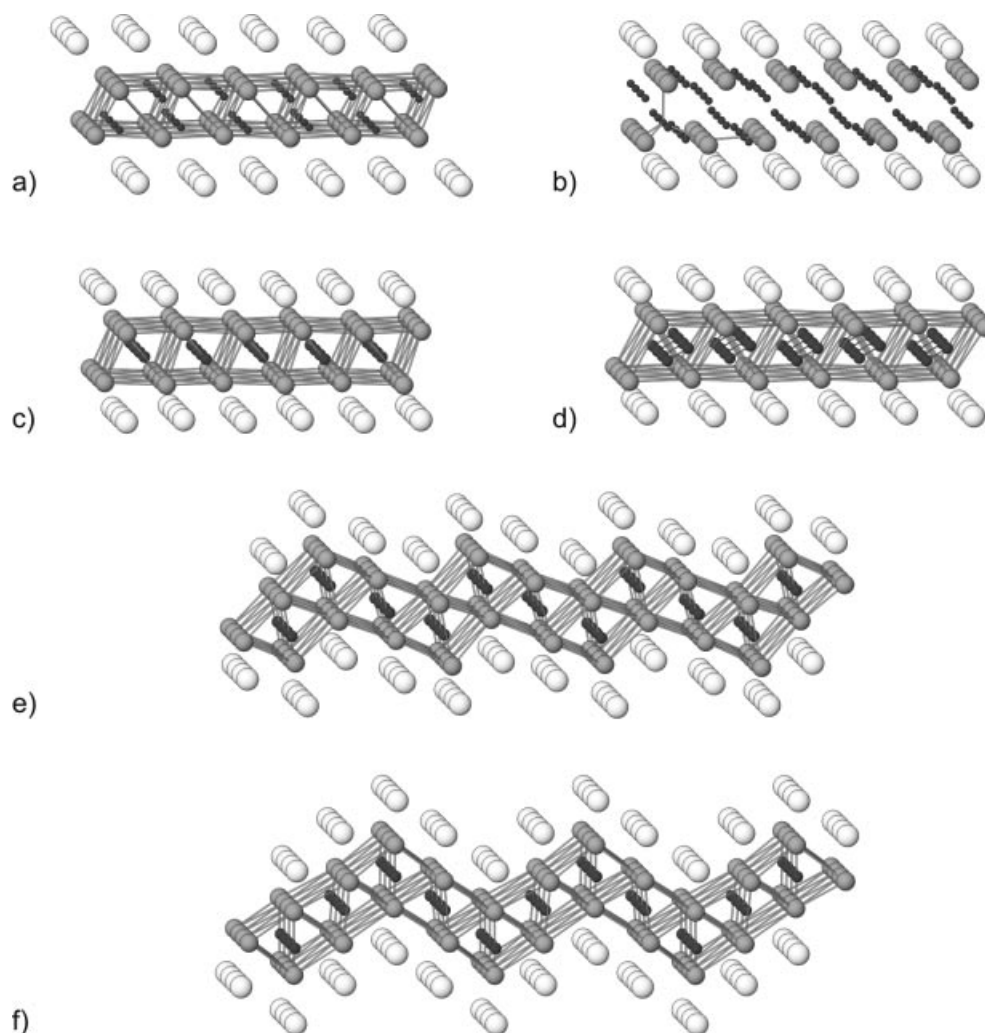


Fig. 5 Layers of condensed Ln_6Z octahedra with interstitial H atoms in (a, b), with C atoms in (c, e, f) and with C_2 units in (d); atoms drawn as in figure 2. Omitting the interconnections between metal atoms in (b) indicates loss of M-M bonding for the composition $\text{Ln}_2\text{H}_4\text{X}_2$.

So far the interstitial atoms and C_2 units are not bonded to each other. This situation as well as the type of building units involved changes when it comes to boride carbide halides. As a rule the B atoms are coordinated by trigonal Ln_6 prisms, and the C atoms lie near the bases of tetragonal Ln_5 pyramids. Some observed examples of layered structures, planar as well as corrugated, formed with B and C as well as a variety of other elements are depicted in figure 7. The two-dimensional networks of Ln atoms host units of different dimensionality with Al-Al, B-B, B-C or Si-Si bonding besides weak Ln-Ln bonding. Graphical representations are limited when it comes to three-dimensional networks. It is needless to say that the structural principles explained here also hold for these structures.

As a final remark, it is noteworthy that we know a plethora of solid state compounds which exhibit M-M bonding between Ln metals, however, so far there is not a single known molecular example. An open field seems to lie ahead of chemists.

3 Interplay of f and d electrons

Metal-rich compounds of the lanthanides provide an extended chemistry of these 4f metals acting as d metals. The d electrons interact via M-M bonds which may be localised in discrete bonds between the atoms or delocalised in extended nets. The f electrons stay away from bonding. They can be treated as core electrons and frequently provide large magnetic moments to the Ln atoms corresponding to e.g. seven unpaired electrons in the case of Gd^{3+} . In spite of the different nature of these electronic systems they strongly interact, a fact that is known since long in the case of metallic systems (RKKY interaction) but also is present in electronically localised systems [14]. Besides this general feature of chemical bonding there are a number of specific conditions found with metal-rich Ln halides which determine the kind of interactions. In many of the structures bonding occurs in discrete clusters, chains and layers and one frequently meets short-range ordering phenomena as it is

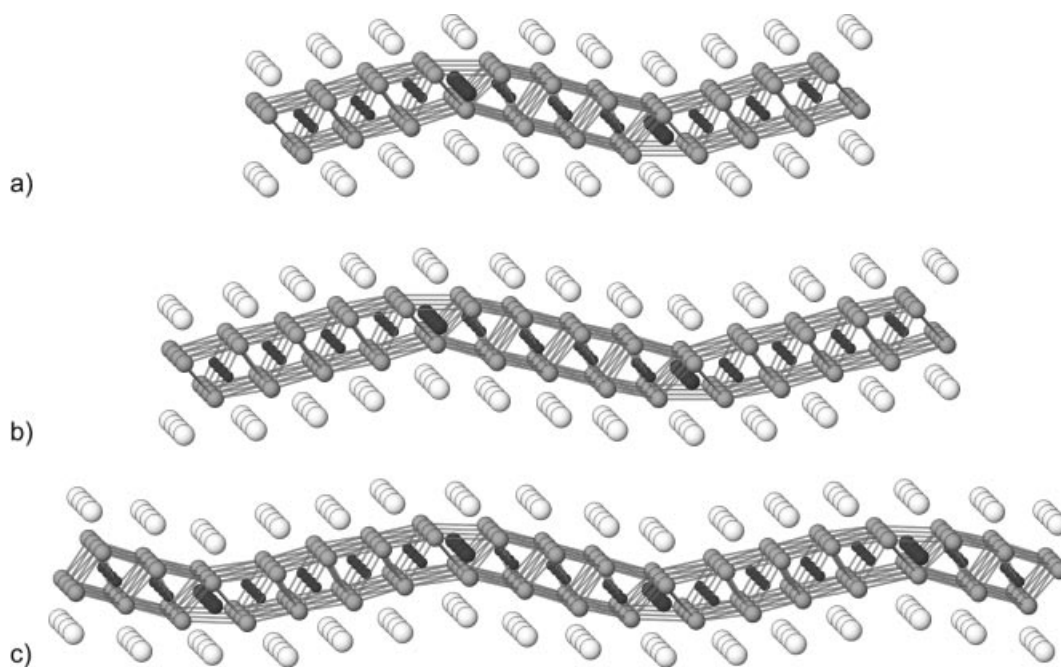


Fig. 6 Layers of condensed Y_6Z octahedra (C centered) and Y_4Z tetrahedra (O centered) in carbide oxide iodides; atoms drawn as in figure 4.

characteristic for low-dimensional systems. Ferro- as well as antiferromagnetic exchange interactions may compete with one another and, due to the fact that the Ln atoms are often arranged in triangles, magnetic frustration effects are liable to occur in the case of antiferromagnetic ordering. The chain compounds Ln_2X_3 (see figure 1) serve as a good example to illustrate the characteristic consequences of all these conditions.

Single crystal neutron diffraction reveals the long-range antiferromagnetic order in Gd_2Cl_3 below 26 K [5]. The magnetic structure determined at 15 K is characterised by ferromagnetic chains of Gd atoms coupled antiferromagnetically across the shared octahedron edges as shown in figure 8. The ordered magnetic moment for the Gd atoms in the octahedron bases, $6\mu_B$, approaches that expected for a $4f^7$ configuration quite in contrast to the nearly vanishing ordered moment of the apical Gd atoms. This observation can be attributed to the fact that the moments located at the apices are magnetically frustrated within each triangle, i.e. the net exchange coupling to the moments in the shared edges nearly cancels. The transition to magnetic order at 26 K is observable in the specific heat as a tiny cusp removing only a small fraction of the magnetic entropy. The majority of the entropy is rather removed in an extended short-range ordering process which leads to a broad hump in the heat capacity reminiscent of the typical behaviour of low-dimensional magnetic systems. This observation strongly supports the view that the exchange coupling within each single chain of octahedra dominates the magnetic properties of Gd_2Cl_3 .

Finally, two examples out of the chemistry of Gd are chosen to illustrate the mutual influence of the d and the f electron systems.

Gadolinium forms the metal-rich carbide halides Gd_2CX ($X = Cl, Br, I$) [15]. The investigations of these compounds are summarised in figure 9. The structure of the iodide consists of double layers of Gd atoms centred by C atoms alternating with single layers of I atoms. One excess electron per formula unit is left. It has d character and is involved in extended M-M bonding within and between the layers of Gd atoms. The compounds Gd_2CX are metallic. Interestingly, the excess electrons can be bound at hydrogen atoms. By reacting the carbide halide with gaseous H_2 these electrons can be “titrated” until the composition of saltlike Gd_2CXH [16] is reached. Neutron diffraction performed on the isostructural deuteride bromide of the neighbouring element Tb leads to the structure also shown in figure 9. The topochemical insertion of H (D) atoms removes M-M bonding, and as expected this chemical change is accompanied by a drastic change in the physical properties. Due to the binding of excess electrons as H^- (D^-) ions the electrical resistance is raised by nearly five orders of magnitude. The pronounced anomaly in the resistance of Gd_2CBr at 120 K is due to the onset of ferromagnetic order within the 4f system. There are distinct differences in the type of magnetic order for $X = Cl$ on one hand and $X = Br, I$ on the other due to different stackings of the Gd_2C layer packages. The Cl atoms are coordinated by trigonal antiprisms of Gd atoms and hence form linear bridges whereas the Br and I atoms form bent bridges due to their trigonal prismatic coordination, resulting in antiferromagnetism in the first and ferromagnetism in the second case. The ordering temperatures are high, 120 K for ferromagnetic Gd_2CBr in contrast to the fully hydrogenated insulating phases Gd_2CHX where magnetic ordering occurs at two orders of magnitude lower temperatures. This difference

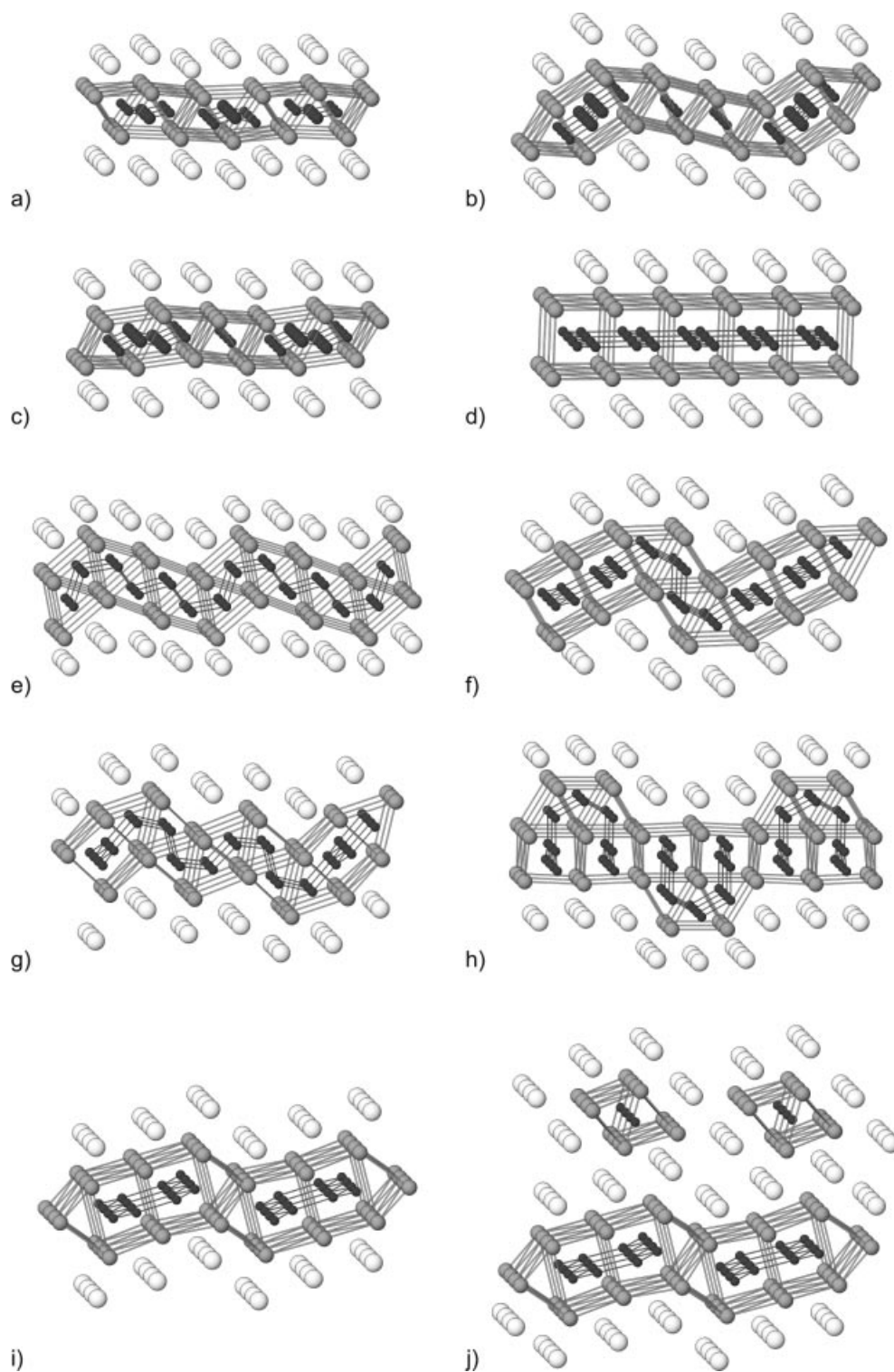


Fig. 7 Layers of condensed Ln_6Z prisms and Ln_5Z square pyramids in boride carbide halides (a-c), and only condensed Ln_6Z prisms in Al, B, Si containing halides (d-i) and with additional chains of Ln_6Z octahedra in (j); atoms drawn as in figure 4.

indicates the strong coupling of the f electron moments via the M-M bonds.

The foregoing example illustrates the influence of the d electron systems on the f electrons. The next example witnesses a remarkable influence in the opposite direction, f

on d electrons. As explained above, GdI_2 crystallises in a structure composed of planar triangular nets of Gd atoms alternating with double layers of I atoms [13]. The simplified description as $\text{Gd}^{3+}\text{I}^{-2}\text{e}^-$ is corroborated by band structure calculations and explains the two-dimensionally

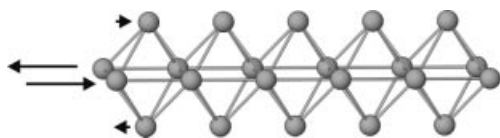


Fig. 8 Magnetic structure of Gd_2Cl_3 at 15 K. The lengths of the arrows correspond to the magnitudes of the ordered moments in different rows of Gd atoms.

metallic character of the compound. The significantly higher metal valence electron concentration compared to Gd_2CX leads to enhanced coupling between the moments of the f electrons with the consequence that GdI_2 becomes ferromagnetic slightly below room temperature [17], $T_c \approx 280$ K, remarkably close to elementary Gd itself. The magnetic ordering is accompanied by a pronounced broad maximum in the electrical resistance shown in figure 10. The calculated electronic band structure revealed a marked anomaly for the conduction bands (van Hove singularity) near to the Fermi level reflecting the two-dimensional character of the system and lead to the prediction of a significant dependence of the resistance on magnetic fields known as colossal magnetoresistance (CMR) which, in fact, could be verified experimentally [18]. Figure 11 shows the pronounced decrease of the resistance in external magnetic fields. The phenomenon is based on an electronically heterogeneous system, where the ferromagnetically ordered localised component polarises the other component represented by the itinerant conduction electrons. Model calculations for GdI_2 indicate that the CMR effect is essentially caused by the polarisation of the d electron system by the f electrons [19]. Colossal magnetoresistance is an intensely investigated phenomenon, not the least because of applicational interests, and it is worth noting that the effect found for GdI_2 at room temperature surpasses that of most CMR materials known, particularly oxomanganates.

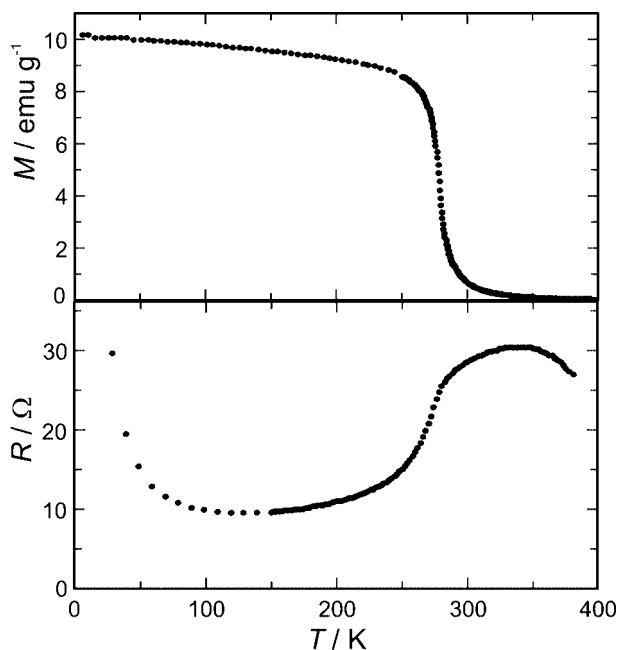


Fig. 10 Magnetic and electrical properties of GdI_2 as a function of temperature, shown in top and bottom, respectively.

There is a broad spectrum of interesting physical properties which result from the interplay of d and f electrons. Some experimental results with GdI_2 may illustrate a tiny part of this spectrum [20, 21]. The compound reversibly absorbs hydrogen up to the composition GdHI_2 which means that the itinerant electrons can be “titrated” as in the case of Gd_2CX . Parallel to the localisation of electrons as H^- ions in GdH_nI_2 the electrical resistance increases with decreasing temperature, and long-range magnetic order is found at lower temperatures than for GdI_2 . This also shifts the CMR effect to lower temperatures, however, with a sig-

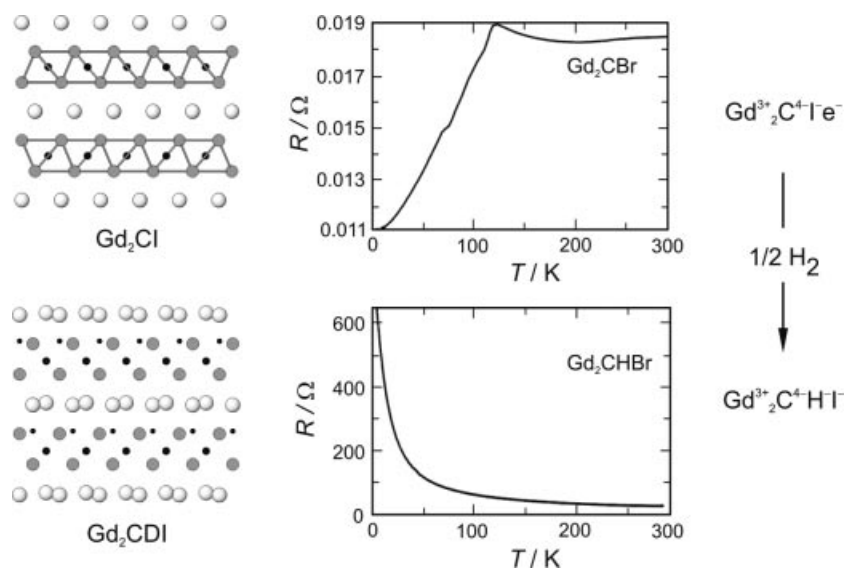


Fig. 9 (left to right) Structures of Gd_2Cl and Gd_2CDI , electrical resistance of the isostructural bromides and schematic description of chemical bonding.

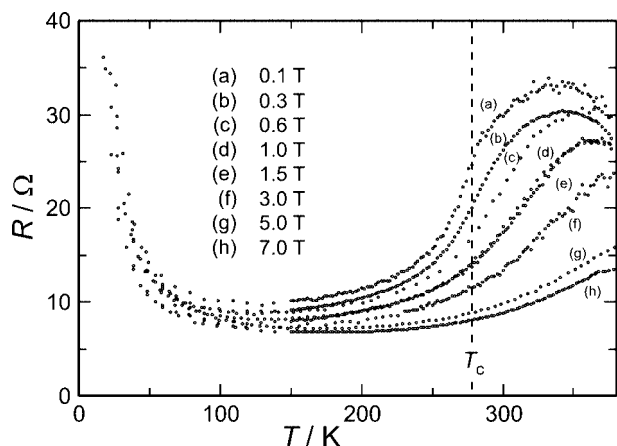


Fig. 11 Influence of external magnetic fields on the electrical resistance of GdI_2 .

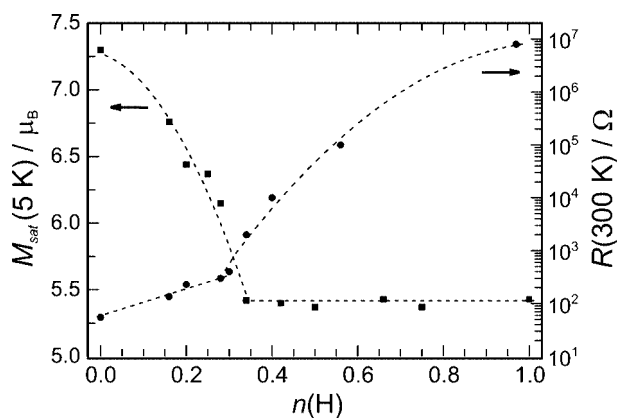


Fig. 12 Magnetic saturation moment and electrical resistance of GdH_nI_2 .

nificant increase of field dependence. More detailed investigations come up with a surprise, see figure 12. Whereas the resistance increases steadily with the hydrogen content n , the magnetic behaviour indicates that the insertion of hydrogen does more than just binding free electrons. Up to $n \approx 1/3$ the saturation moment decreases continuously and then remains almost constant with further increase of the H content. This behaviour is caused by the fact that the H atom induces antiferromagnetic instead of ferromagnetic interaction between the immediately surrounding Gd atoms. As a result, the spin configuration in the triangular Gd_3H units becomes geometrically frustrated, because in a triangle only two antiparallel moments are possible besides one parallel. The frustrated configuration of all magnetic sites is reached at $n = 1/3$, as shown for the structurally ordered layer in figure 13, where now each Gd^{3+} ion experiences competing magnetic interactions. Further insertion of H atoms does not change the magnetic state considerably except for influencing the ratio of ferromagnetic and antiferromagnetic interactions and decreasing the free carrier concentration.

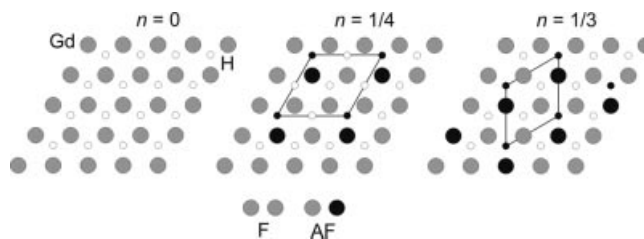


Fig. 13 (left to right) Ferromagnetic order in a Gd atom layer of GdI_2 with empty H atom positions; representation of structurally ordered layers with ferro- and antiferromagnetic interactions (F, AF) in $\text{GdH}_{0.25}\text{I}_2$ and $\text{GdH}_{0.33}\text{I}_2$, respectively. The system is completely frustrated for the latter composition.

Many materials with frustrated magnetic lattices do not undergo phase transitions to a long range ordered state but rather exhibit spin-freezing effects at low temperatures. This is also the case for the GdH_nI_2 system. Samples within the range of n from $1/3$ to $2/3$ show spin glass-like behaviour below a freezing temperature T_f , as evidenced by a characteristic thermal hysteresis in the dc magnetic susceptibilities as well as frequency shifts of T_f . Here, it is interesting to note that in contrast to many known spin glasses in which the frozen spin configuration is caused by site disorder in the magnetic sublattices, the disorder in GdH_nI is introduced in the diamagnetic H atom sublattice.

Conclusions

The chosen examples provide some impression of a broad research area based on a d metal chemistry of the 4f elements, comprising a plethora of new compounds and a wealth of interesting physical phenomena. These cover electronic localisation / delocalisation with metal-to-insulator transitions, superconductivity in the case of non-magnetic phases – in the latter case mimicking the “true” d metal yttrium – and magnetic order as well as inhibited order in low-dimensional systems. We have chosen some magnetic phenomena in this review as a reverence to *Wilhelm Klemm* whose name is intimately associated with the development of magneto chemistry.

References

- [1] W. Klemm, H. Bommer, *Z. Anorg. Allg. Chem.* **1937**, 231, 138–171.
- [2] D. A. Lokken, J. D. Corbett, *Inorg. Chem.* **1973**, 12, 556–559.
- [3] A. Simon, N. Holzer, Hj. Mattausch, *Z. Anorg. Allg. Chem.* **1979**, 456, 207–216.
- [4] G. Meyer, *Chem. Rev.* **1988**, 88, 93–107.
- [5] A. Simon, Hj. Mattausch, G. J. Miller, W. Bauhofer, R. K. Kremer, in: *Handbook on the Physics and Chemistry of Rare Earth*, Vol 15, K. A. Gschneidner, Jr. and L. Eyring (eds), Elsevier Science Publishers, Amsterdam-London-New York-Tokyo **1991**, pp. 191–285.
- [6] J. D. Corbett, *J. Chem. Soc., Dalton Trans.* **1996**, 575–587.
- [7] A. Simon, M. Göbel, R. Eger, Hj. Mattausch, unpublished **2005**.

- [8] U. Beck, *Dissertation*, Univ. Stuttgart **1995**.
- [9] J. D. Martin, J. D. Corbett, *Angew. Chem.* **1995**, *107*, 234–236; *Angew. Chem. Int. Ed. Engl.* **1995**, *34*, 233–235.
- [10] M. Ryazanov, L. Kienle, A. Simon, Hj. Mattausch, *Inorg. Chem.* **2006**, *45*, 2068–2074.
- [11] H. Schäfer, H. G. Schnering, *Angew. Chem.* **1964**, *76*, 833–848.
- [12] A. Simon, *Angew. Chem.* **1988**, *100*, 163–188; *Angew. Chem. Int. Ed. Engl.* **1988**, *27*, 159–183.
- [13] E. Warkentin, H. Bärnighausen, *Z. Anorg. Allg. Chem.* **1979**, *459*, 187–200.
- [14] L. Roy, T. R. Hughbanks, *J. Solid State Chem.* **2003**, *176*, 294–305.
- [15] C. Bauhofer, Hj. Mattausch, G. J. Miller, W. Bauhofer, J. K. Cockcroft, R. K. Kremer, A. Simon, *J. Less-Common Met.* **1990**, *167*, 65–79.
- [16] M. Ruck, A. Simon, *Z. Anorg. Allg. Chem.* **1992**, *617*, 7–18.
- [17] C. Michaelis, W. Bauhofer, H. Buchkremer-Hermanns, R. K. Kremer, G. J. Miller, A. Simon, *Z. Anorg. Allg. Chem.* **1992**, *618*, 98–106.
- [18] C. Felser, K. Ahn, R. K. Kremer, R. Seshadri, A. Simon, *J. Solid State Chem.* **1999**, *147*, 19–25.
- [19] I. Eremin, P. Thalmeier, P. Fulde, R. K. Kremer, K. Ahn, A. Simon, *Phys. Rev. B* **2001**, *64*, 064425-1-6.
- [20] M. Ryazanov, A. Simon, R. K. Kremer, Hj. Mattausch, *J. Solid State Chem.* **2005**, *178*, 2339–2345.
- [21] M. Ryazanov, A. Simon, R. K. Kremer, Hj. Mattausch, *Phys. Rev. B* **2005**, *72*, 092408-1-4; M. Ryazanov, *Dissertation*, Univ. Stuttgart **2004**.
- [22] T. R. Hughbanks, J. D. Corbett, *Inorg. Chem.* **1988**, *27*, 2022–2026.
- [23] Hj. Mattausch, C. Hoch, A. Simon, *Z. Anorg. Allg. Chem.* **2005**, *631*, 1423–1429.
- [24] H. Artelt, T. Schleid, G. Meyer, *Z. Anorg. Allg. Chem.* **1992**, *618*, 18–25.
- [25] D. S. Dudis, J. D. Corbett, *Inorg. Chem.* **1987**, *26*, 1933–1940.
- [26] T. R. Hughbanks, J. D. Corbett, *Inorg. Chem.* **1989**, *28*, 631–635.
- [27] D. J. Hinz, G. Meyer, *Z. Kristallogr. NCS* **1995**, *210*, 958.
- [28] E. Warkentin, R. Masse, A. Simon, *Z. Anorg. Allg. Chem.* **1982**, *491*, 323–336.
- [29] S. Uhrlandt, H. Artelt, G. Meyer, *Z. Anorg. Allg. Chem.* **1994**, *620*, 1532–1536.
- [30] Hj. Mattausch, E. Warkentin, O. Oeckler, A. Simon, *Z. Anorg. Allg. Chem.* **2000**, *626*, 2117–2124.
- [31] M. Lulei, J. D. Martin, L. M. Hoistad, J. D. Corbett, *J. Am. Chem. Soc.* **1997**, *119*, 513–520.
- [32] M. Lulei, P. A. Maggard, J. D. Corbett, *Angew. Chem.* **1996**, *108*, 1798–1799; *Angew. Chem. Int. Ed. Engl.* **1996**, *35*, 1704–1705.
- [33] H. M. Artelt, G. Meyer, *Z. Anorg. Allg. Chem.* **1993**, *619*, 1–6.
- [34] Hj. Mattausch, A. Simon, L. Kienle, C. Hoch, C. Zheng, R. K. Kremer, *Z. Anorg. Allg. Chem.*, in print **2006**.
- [35] Hj. Mattausch, G. V. Vajenine, O. Oeckler, R. K. Kremer, A. Simon, *Z. Anorg. Allg. Chem.* **2001**, *627*, 2542–2546.
- [36] S. J. Steinwand, J. D. Corbett, *Inorg. Chem.* **1996**, *35*, 8056–8067.
- [37] S. M. Kauzlarich, T. Hughbanks, J. D. Corbett, P. Klavins, R. H. Shelton, *Inorg. Chem.* **1988**, *27*, 1791–1797.
- [38] Hj. Mattausch, O. Oeckler, A. Simon, *Z. Kristallogr. NCS* **2003**, *218*, 282.
- [39] S.-J. Hurn, J. D. Corbett, *J. Solid State Chem.* **1986**, *64*, 331–346.
- [40] H. Ließ, H.-J. Meyer, G. Meyer, *Z. Anorg. Allg. Chem.* **1996**, *622*, 494–500.
- [41] Hj. Mattausch, O. Oeckler, A. Simon, *Inorg. Chim. Acta* **1999**, *289*, 174–190.
- [42] S.-Y. Hwu, D. S. Dudis, J. D. Corbett, *Inorg. Chem.* **1987**, *26*, 469–473.
- [43] Hj. Mattausch, O. Oeckler, A. Simon, *Z. Kristallogr. NCS* **2000**, *215*, 199.
- [44] O. Oeckler, L. Kienle, Hj. Mattausch, A. Simon, *Angew. Chem.* **2002**, *114*, 4431–4433; *Angew. Chem. Int. Ed.* **2002**, *41*, 4257–4259.
- [45] O. Oeckler, L. Kienle, Hj. Mattausch, V. Jarchow, A. Simon, *Z. Kristallogr.* **2003**, *218*, 321–331.
- [46] Hj. Mattausch, R. K. Kremer, A. Simon, W. Bauhofer, *Z. Anorg. Allg. Chem.* **1993**, *619*, 741–747.
- [47] M. W. Payne, P. K. Dorhout, S.-J. Kim, T. R. Hughbanks, J. D. Corbett, *Inorg. Chem.* **1992**, *31*, 1389–1394.
- [48] S.-Y. Hwu, J. D. Corbett, K. R. Poeppelmeier, *J. Solid State Chem.* **1985**, *57*, 43–58.
- [49] S. M. Kauzlarich, M. W. Payne, J. D. Corbett, *Inorg. Chem.* **1990**, *29*, 3777–3781.
- [50] M. Ruck, A. Simon, *Z. Anorg. Allg. Chem.* **1992**, *617*, 7–18.
- [51] F. Ueno, K. R. A. Ziebeck, Hj. Mattausch, A. Simon, *Rev. Chim. Miner.* **1984**, *21*, 804–808.
- [52] Hj. Mattausch, W. Schramm, R. Eger, A. Simon, *Z. Anorg. Allg. Chem.* **1985**, *530*, 43–59.
- [53] U. Schwanzitz-Schüller, A. Simon, *Z. Naturforsch.* **1985**, *40b*, 710–716.
- [54] T. Schleid, G. Meyer, *Z. Kristallogr.* **1994**, *209*, 371.
- [55] Hj. Mattausch, R. Eger, A. Simon, *Z. Anorg. Allg. Chem.* **1991**, *597*, 145–150.
- [56] Hj. Mattausch, R. K. Kremer, R. Eger, A. Simon, *Z. Anorg. Allg. Chem.* **1997**, *623*, 619–622.
- [57] Hj. Mattausch, A. Simon, *J. Less-Common Met.* **1985**, *113*, 149–155.
- [58] C. Bauhofer, Hj. Mattausch, R. K. Kremer, A. Simon, *Z. Anorg. Allg. Chem.* **1995**, *621*, 1501–1507.
- [59] A. Simon, C. Schwarz, W. Bauhofer, *J. Less-Common Met.* **1988**, *137*, 343–351.
- [60] Hj. Mattausch, O. Oeckler, C. Zheng, A. Simon, *Z. Anorg. Allg. Chem.* **2001**, *627*, 1523–1531.
- [61] C. Zheng, A. Simon, Hj. Mattausch, *J. Alloys Comp.* **2002**, *338*, 165–172.
- [62] C. Zheng, Hj. Mattausch, A. Simon, *Z. Kristallogr. NCS* **2001**, *216*, 495–496.
- [63] A. Simon, T. Koehler, *J. Less-Common Met.* **1986**, *116*, 279–292.
- [64] U. Schwanzitz-Schüller, A. Simon, *Z. Naturforsch.* **1985**, *40b*, 705–709.
- [65] Hj. Mattausch, H. Borrmann, R. Eger, R. K. Kremer, A. Simon, *Z. Anorg. Allg. Chem.* **1994**, *622*, 1889–1897.
- [66] Hj. Mattausch, H. Borrmann, A. Simon, *Z. Naturforsch.* **1993**, *48b*, 1828–1830.
- [67] G. Meyer, H. Mattfeld, K. Kraemer, *Z. Anorg. Allg. Chem.* **1993**, *619*, 1384–1388.
- [68] P. O. Jeitschko, Hj. Mattausch, A. Simon, *Z. Anorg. Allg. Chem.* **1997**, *623*, 1889–1897.
- [69] O. Oeckler, Hj. Mattausch, A. Simon, *Z. Anorg. Allg. Chem.* **1998**, *642*, 1834–1838.
- [70] Hj. Mattausch, O. Oeckler, G. V. Vajenine, R. K. Kremer, A. Simon, *Solid State Sciences* **1999**, *t1*, 509–521.

- [71] O. Oeckler, V. Duppel, Hj. Mattausch, A. Simon, *Inorg. Chem.* **1999**, *38*, 1767–1771.
- [72] Hj. Mattausch, A. Simon, C. Felser, R. Dronskowski, *Angew. Chem.* **1996**, *108*, 1805–1807; *Angew. Chem. Int. Ed. Engl.* **1996**, *35*, 1685–1687.
- [73] Hj. Mattausch, A. Simon, *Angew. Chem.* **1995**, *107*, 1764–1766; *Angew. Chem. Int. Ed. Engl.* **1995**, *34*, 1633–1635.
- [74] Hj. Mattausch, O. Oeckler, A. Simon, *Z. Anorg. Allg. Chem.* **1999**, *625*, 297–301.
- [75] Hj. Mattausch, A. Simon, *Angew. Chem.* **1998**, *110*, 498–501; *Angew. Chem. Int. Ed. Engl.* **1998**, *37*, 499–502.
- [76] O. Oeckler, Hj. Mattausch, A. Simon, *Z. Anorg. Allg. Chem.* **2005**, *631*, 3013–3018.
- [77] Hj. Mattausch, O. Oeckler, C. Hoch, A. Simon, *Z. Anorg. Allg. Chem.*, in print **2006**.
- [78] S. Uhrlandt, Th. Heuer, G. Meyer, *Z. Anorg. Allg. Chem.* **1995**, *621*, 1299–1303.
- [79] G. Meyer, S. Uhrlandt, *Angew. Chem.* **1993**, *105*, 1379–1381; *Z. Anorg. Allg. Chem.* **1994**, *620*, 1872–1878.